Development and application of limiter Langmuir probe array on EAST

S.C. Liu[a, *], L. Liao[a, b], W.Y. Wei[a, b], Y. Liang[a,c, *], J. C. Xu[d], L. Cao[a], S. Li[a], L. Li[a], L.Y. Meng[a, b], J.P. Qian[a], Q. Zang[a], L. Wang[a], S. Xu[c], J. Cai[a], N. Yan[a], Q. Ma[a, b], N. Zhao[e], R. Chen[a], G.H. Hu[a], J.B. Liu[a], X.J. Liu[a], T.F. Ming[a], L.T. Li[a, f], Y. Sun[a], L. Zeng[a], G.Q. Li[a], D.M. Yao[a], G.S. Xu[a], X.Z. Gong[a], X. Gao[a] and EAST Team

[a] Institute of Plasma Physics, Chinese Academy of Sciences, Hefei 230031, Peoples Republic of China

[b] University of Science and Technology of China, Hefei, 230026, Peoples Republic of China

[c] Forschungszentrum Jülich GmbH, Institut für Energie - und Klimaforschung - Plasmaphysik, Partner of the Trilateral Euregio Cluster (TEC), 52425 Jülich, Germany

[d] School of Mechanical Engineering, Anhui University of Science & Technology, Huainan 232001, China

[e] School of Science, Southwest University of Science and Technology, Mianyang 621010, China

[f] Anhui University, Hefei 230039, People's Republic of China

E-mail: shaocheng.liu@ipp.ac.cn; y.liang@fz-juelich.de

Abstract

A newly developed limiter Langmuir probe (LLP) array has been applied to the scrape-off layer (SOL) plasma measurement in EAST tokamak. The LLP system consists of two poloidal arrays located at opposite sides of the low field side guard limiter, and each poloidal array has 26 Langmuir probe channels with a spatial resolution of 35 mm in the vertical direction. The probe tip is polished to match the local graphite tile plane and avoid the leading edge and the corresponding high heat load. The probe can be assembled easily and has good electric insulating property. Langmuir probes have three operation modes, i.e., floating potential mode, Mach probe mode, and single probe mode. The LLP array could be operated in different modes according to the experimental purpose. The LLP array has been successfully applied to the EAST experiment in 2021, and measure the three-dimensional plasma structure in the SOL.

Keywords: limiter probe, Langmuir probe, scrape-off layer, EAST, tokamak, plasma

1. Introduction

The plasma-wall interaction is a critical issue in the magnetically confined devices and has a considerable impact on the performance of fusion plasma and the lifetime of the plasma-facing components in the next step burning plasma experiments [1]. The edge plasma parameters, such as plasma potential, electron temperature and density, are important to characterize the plasma conditions, and interpret the physics of edge transport and the interaction between plasma and materials [2, 3]. Usually, the edge electron temperature and density can be measured by Langmuir probe [4], edge Thomson scattering [5], beam emission spectroscopy [6], and lithium beam[7] *et al*. Owing to the easily manufacture and flexible pins arrangement, Langmuir probes are widely applied to the edge plasma measurement in tokamaks and stellarators. Reciprocating probe is used to measure the edge radial profiles of plasma parameters, such as temperature, density, parallel flow velocity and turbulence behaviors [8-10]. In divertor region, Langmuir probes embedded in the target plate could measure not only the electron temperature and density, but also the particle flux that is an important criterion of divertor detachment, consequently divertor Langmuir probes have been installed in many devices, such as JET [11], DIII-D[12], JT-60 [13], EAST [14, 15], KSTAR [16] and W7-X [17]. In tokamak and stellarator, a guard limiter is used to confine the hot plasma and protect the in-vessel components behind it. Although the limiter is located in the far scrape-off layer (SOL), strong heat load deposited on the limiter surface is observed by the visible camera and infra-red camera [18, 19], indicating the interaction between SOL plasma and limiter. Since the SOL plasma reveals clear three-dimensional patterns under some conditions in tokamaks, e.g. the eruption of edge localized mode (ELM) and the application of resonant magnetic perturbation (RMP) [20-22], it makes sense to measure the plasma parameters in the upstream SOL by using fixed Langmuir probes at the guard limiter and the divertor plasma by using divertor Langmuir

probes, which is beneficial to the understanding of three-dimensional SOL physics. Limiter Langmuir probe (LLP) has been installed in some tokamaks, such as JET [23], Alcator C-Mod [24] and J-TEXT [25], and the corresponding application includes ELM propagation and SOL current measurement driven by biasing electrode. LLP has been also applied to the edge plasma measurement in stellarator, such as W7-AS and W7-X [26, 27]. To study the 3D edge physics, a new limiter Langmuir probe array is developed in EAST. The rest of this paper is organized as follows. The engineering design of LLP is given in section 2. The electric circuit setup and commissioning experimental results are presented in section 3. Section 4 is a summary.

2. Engineering design of LLP

EAST is a superconducting tokamak with a major radius $R_0 = 1.9$ m, and a minor radius $a \leq 0.45$ m [28]. The guard limiter is located on the low field side and in the middle of ports G and H. Because a new RMP coil located behind the limiter is under development [29], it is important to measure the 3D plasma structure induced by RMPs near the coil. In consequence, the limiter Langmuir probes with two poloidal arrays are developed in 2020, and have been operated since 2021. The LLP array could measure the poloidal structure of SOL plasma, including floating potential, ion saturation current, electron density, temperature, particle and heat fluxes.

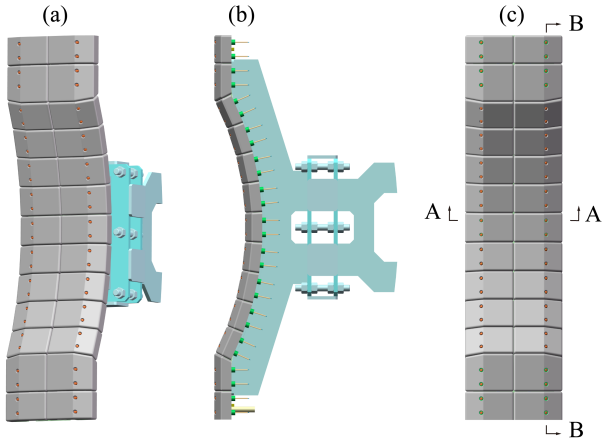

Fig. 1. The mechanical design diagrams of LLPs and limiter after assembly. (a) 3D view; (b) side view; (c) front view. The probe tips are shown in orange. In panel (c), the cut faces of two cutaway views A-A and B-B are illustrated.

The limiter consists of graphite tiles in the front, heat sink in the middle and stainless-steel support bracket in the back, as shown in Fig. 1. The middle part of the limiter front surface has a circular arc shape that is the same as the last closed flux surface (LCFS) on the low field side, while the front surface is vertical at the top and bottom in order to avoid protrusion. The height of limiter is 950 mm, and the width (toroidal direction) is 240 mm. The front tiles are made from a type of doped graphite, with high thermal conductivity up to 180 W/mK, bending strength larger than 40 MPa, and compressive strength larger than 80 MPa [30]. After manufacture, the graphite tiles are coated with a SiC layer to improve the performance of material and prolong its left time [31]. There are 26 graphite tiles in the limiter, with 13 tiles on both the left and right sides. For the purpose of avoiding the leading edge and the corresponding high heat load, there is an angle ($\theta = 20°$) between the two front surfaces of a graphite tile, as illustrated in Fig. 2. The graphite tiles are bolted to the active water-cooling heat sink that is made from chromium zirconium copper (CuCrZr). There are two vertical cooling tubes inside the heat sink, each with a diameter of 12 mm. The cooling water mass flow rate is 3 t/h, and the corresponding speed is 7.3 m/s. At the top of the graphite tile bevel, there is a hole with a diameter of 8.5 mm, and at the same radial position, the heat sink also has a stepped hole, as displayed in Fig. 2. Note that at the bottom of this stepped hole it is an internal thread, aiming to clamp the probe assembly at the end. The major radius of the limiter is $R = 2350$ mm at the outer midplane ($Z = 0$).

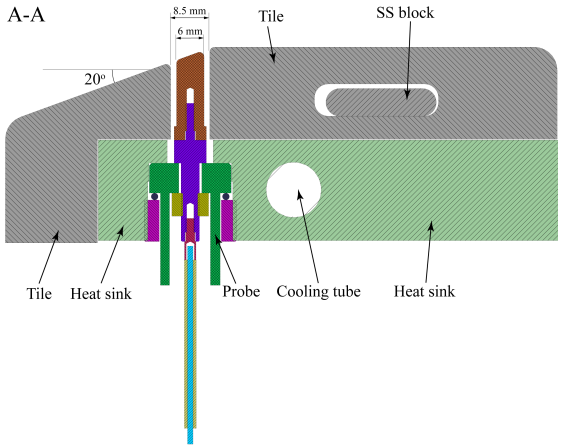

Fig. 2. Cutaway view of A-A with cut face shown in Fig. 1 (c).

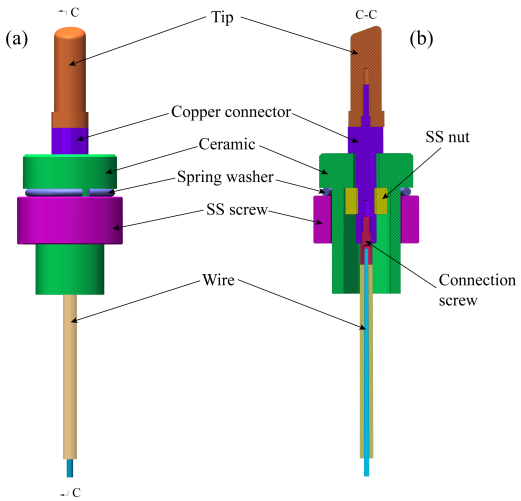

Fig. 3. (a) the 3D drawing of an LLP. (b) Cutaway view C-C with cut face shown in (a).

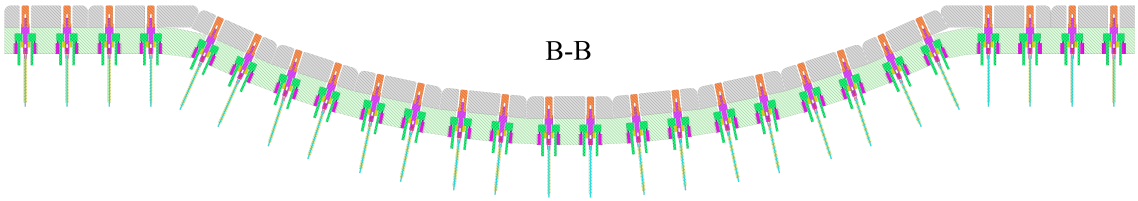

Fig. 4. Cutaway view of B-B with cut face shown in Fig. 1 (c).

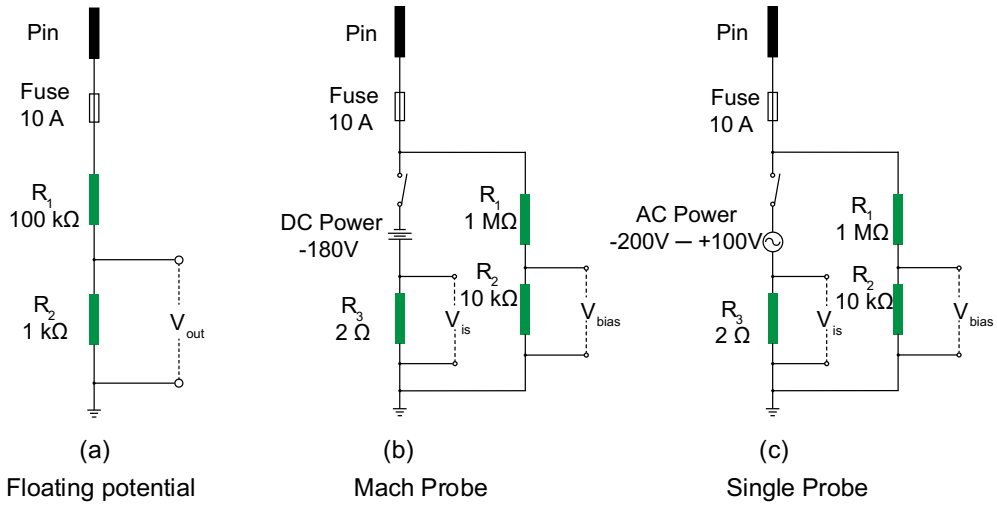

Fig. 5. Electric circuit of LLP. (a) Floating potential circuit; (b) Mach probe circuit; (c) single probe circuit.

An LLP is composed of graphite tip, copper connector, ceramic holder, spring washer, stainless steel (SS) screw, SS nut, connection screw and wire, as illustrated in Fig. 3. A similar engineering structure has also been applied to the divertor Langmuir probe in EAST [32]. The probe tip is made from the EDM-4 graphite, with bending strength 120 Mpa, compressive strength 148 Mpa, hardness 76 Shore, and electrical resistivity 12.7 μΩm. The graphite tip is a cylinder with a diameter of 6 mm, and the front surface is polished to match the plane of graphite tile bevel, as shown in Fig. 2. The bottom of the probe tip has a threaded hole, which is connected with the copper connector through the bolt-nut thread connection. The copper connector can be divided into three parts from front to back: the first part is a small bolt connected with the graphite tip; the middle part is a square nut with the largest diameter which will be used to fix the copper connector to the ceramic holder; the third part has external thread outside connected with the SS nut and a threaded hole inside connected with the connection screw. The front part of the copper connection screw is a bolt, and the back part has a small blind hole inside. The wire and the copper connection screw are crimped together by a wire crimper which could sustain a much higher temperature than soldering. The plasma signal is transmitted by the graphite tip, copper connector, connection screw and wire. The cylindrical ceramic holder made from Al_2O_3 is sintered up to 1700 °C by using hot-press pour-casting technology with a specially designed mock-up model, and it isolates the electroconductive components (tip, copper connector, connection screw, wire and SS nut) from the other components of the probe and the heat sink. Inside the ceramic holder, there is a stepped hole with a small circular hole in the front and a large square hole in the back. The SS nut has a threaded hole in the center and a square appearance outside. The external surface of the ceramic holder is a stepped cylinder, with the diameter of the front part a bit larger. The tailor-made spring washer is used to prevent the connection from becoming loose.

The Langmuir probe can be assembled in the laboratory with the following procedures. As illustrated in Fig. 3, in the beginning, crimp the wire with the connection screw, and then connect the connection screw to the copper connector through the bolt-nut method. Put the SS nut into the square hole of the ceramic holder, and then screw the copper connector into the SS nut from the front side by rotating the middle nut of the copper connector, finally screw up the probe tip with the copper connector. As shown in Fig. 2, after this preliminary assembly, insert the Langmuir probe into the stepped hole in the heat sink from the backside, next put the spring washer into this hole, and finally push the SS screw into the threaded hole to clamp the LLP assembly. The last step is to polish the graphite tip in order to ensure that its front surface is on the same plane as the graphite tile bevel. When all the LLPs are installed in the limiter, the cutaway view of B-B is shown in Fig. 4 with the cut face displayed in Fig. 1 (c). We can see every LLP is in the same plane of graphite tile. The spatial resolution of each LLP poloidal array is about 35 mm. The

sampling rate of the data acquisition (DAQ) system can be up to 2 MHz. Based on the high temporal and spatial resolution, the LLP array can measure the fast response of SOL plasma, the corresponding poloidal structure, and the asymmetry between two toroidal directions.

The design of LLP has several advantages. Firstly, the assembly process is simple and easy to carry out. Secondly, the electroconductive components transmitting plasma signal are connected firmly through bolt-nut connection and crimped connection. Consequently, the measured parameter is reliable in long-term operation. Thirdly, the electric insulating property of the probe is good, because all the electroconductive components are isolated from the surrounding heat sink and graphite tile by the ceramic holder. Fourthly, the probe tip can be taken out from the front side when the probe tip needs maintenance during the interval of experimental campaigns.

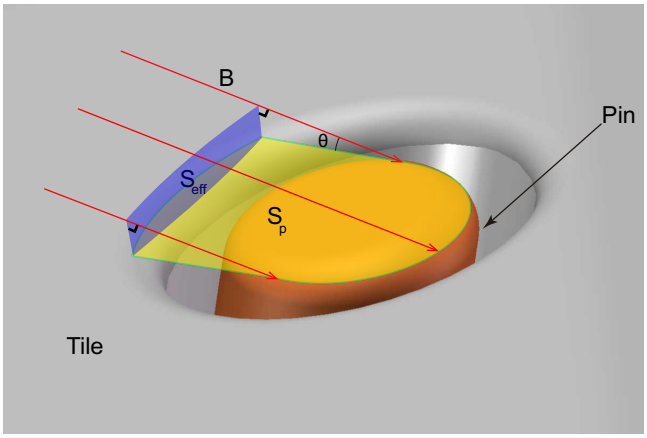

Fig. 6. Schematic of the probe effective collecting area. The probe tip is in orange, and the graphite tile is in grey. The effective collecting area perpendicular to the magnetic field line is shown in blue.

3. Commissioning experiment of LLP

The LLP array has been commissioned during the first experimental campaign of EAST in 2021. In this section, the experimental setup of the LLP system and some preliminary results will be presented.

3.1 Electric circuit

The LLP system has two poloidal arrays, each with 26 probes. There are three types of LLP electric circuits, including floating potential circuit, Mach probe circuit and single probe circuit, as illustrated in Fig. 5. As the name implies, the floating potential circuit is used to measure floating potential, with the sampling resistance of $R_2/R_1 = 1$ kΩ/100 kΩ. Note that the circuit ground is connected to the vessel of EAST tokamak. A glass fuse of 10 A is connected in series to the probe, aiming to protect the circuit and the DAQ system. The Mach probe circuit is used to measure the ion saturation current. The sampling resistance is 2 Ω for the current measurement. In this commissioning experiment, the DC power supply is provided by a -180 V battery pack consisting of twenty 9 V batteries. The variation of biasing voltage is measured by a parallel circuit with the sampling resistance of $R_2/R_1 = 10$ kΩ/1 MΩ. The single probe circuit, measuring the electron temperature and density, is the same as the Mach probe circuit except that the DC power is replaced by an AC power. Since every probe works independently, the circuit setup of LLP array can be adjusted optimally according to the purpose of experimental proposal. With these three types of circuits, the floating potential, ion saturation current, electron temperature and density in the SOL can be measured at the same time.

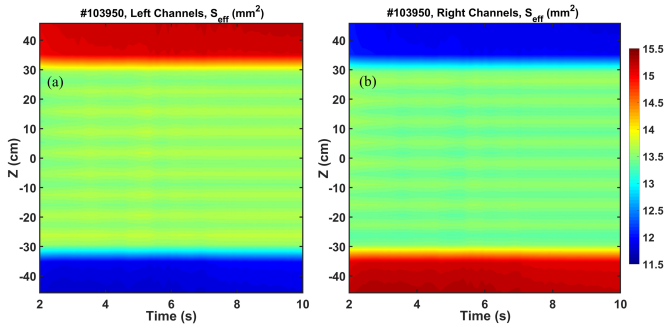

Fig. 7. Temporal evolution of the effective collecting area of discharge 103950 for the left LLP array (a) and the right LLP array (b).

3.2 Effective collecting area

The LLP effective collecting area S_{eff} is necessary for the calculation of ion saturation current density and electron density. The schematic of the S_{eff} calculation is illustrated in Fig. 6. All the field lines arriving at the probe tip enclose the blue shaded region which is perpendicular to the magnetic field, and consequently the area of this region is the effective collecting area S_{eff}. The angle between the incident magnetic field and the tile plane is θ, therefore the effective collecting area can be derived by $S_{eff} = S_p sin\theta$, where S_p is the area of the yellow shaded region from which the field lines could reach the pin rather than the inner wall of graphite tile, as shown in Fig. 6. The magnetic field is obtained from the EFIT equilibrium [33]. The coordinates of the graphite tile vertices and the probe tip are measured by the laser tracker system when the installation was finished inside the vacuum chamber [34]. The effective collecting area S_{eff} of a typical discharge 103950 is presented in Fig. 7 for both the left and right LLP arrays. In the circular-arc-shaped region, both the left and right LLP channels have similar $S_{eff} = 13.3 - 13.7$ mm^2, i.e., the variation of S_{eff} is negligible. This is mainly due to the almost constant incident angle θ. It should be pointed out that the small oscillation of S_{eff} in the vertical direction is caused by the two adjacent channels located in the same graphite tile, because both channels have the same normal direction of the tile plane but different magnetic fields due to the vertical

coordinate difference between the two probe tips. In the left poloidal array, the S_{eff} of the top four LLP channels is about 15.2 mm^2, while the S_{eff} is about 11.8 mm^2 for the bottom four channels, because their graphite tiles are vertical and located behind the flux surface of the central circular arc region. The top and bottom channels of the right LLP array reveal the same features of S_{eff}, but the bottom S_{eff} is larger than that at the top. Since the variation of the effective collecting area is almost constant in the central circular arc region, it is convenient to derive current density from the measured ion saturation current.

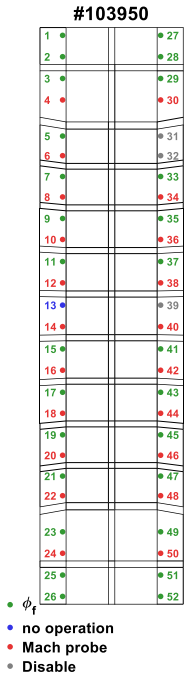

Fig. 8. Circuit setup of LLP array for discharge 103950.

3.3 Preliminary experimental results

The ion saturation current denoting parallel particle flux is an important physical quantity to characterize the SOL plasma structure, as reported in previous publications [35, 36]. Firstly, the poloidal structure of ion saturation current density measured by the LLP array is presented in Fig. 9 during a rotating RMP experiment. The discharge 103950 is an Ohmic discharge, with plasma current $I_p = 500$ kA, line-integrated electron density $n_{el} = 10^{19}$ m^{-2}, and toroidal field 2.24 T at the plasma center. The RMP is rotated with a frequency of 1 Hz, maximum RMP coil current of 1.6 kA, and the phase difference between the upper and lower RMP coils $\delta\phi_{UL} = 0$, as shown in Fig. 9 (a) and (b). The electric circuit setup of all the LLPs is illustrated in Fig. 8, and 21 LLP channels are used to measure the ion saturation current. The measured ion saturation current density j_{is} is shown in Fig. 9 (c) and (d). When the RMP coil current increases from $t = 3$ s and reaches its maximum at $t = 3.5$ s, the peak ion saturation current density j_{is} shifts from $Z < 0$ to $Z > 0$. During the time of $t = 3.5 - 4$ s, the RMP coil currents are constant, and the ion saturation current density j_{is} at the limiter is also stable. Note that the three bright bands during this period are induced by the supersonic molecular beam injection (SMBI). When the RMP coil currents rotate for the first cycle, the position of the peak j_{is} decreases slowly from $Z \approx 15$ cm to -20 cm from $t = 4$ s to 4.5 s; then the ion saturation current density j_{is} is close to zero in the whole limiter from $t = 4.5$ s to 4.9 s, indicating the deposition of particle flux on the limiter is very weak; from $t = 4.9$ s to 5 s, the current density j_{is} appears again in the limiter with the main particle deposition located at $Z \approx 15$ cm. During the second cycle ($t = 5 - 6$ s) of RMP rotation, the ion saturation current density exhibits the same temporal evolution and spatial structure, and the value j_{is} is a bit larger than that in the first cycle. These cyclic variations of j_{is} demonstrate that the SOL plasma response to RMPs is three-dimensional and rotated synchronously with the RMPs. This observation also confirms that the LLP array can measure the poloidal structure of SOL plasma with high sensitivity.

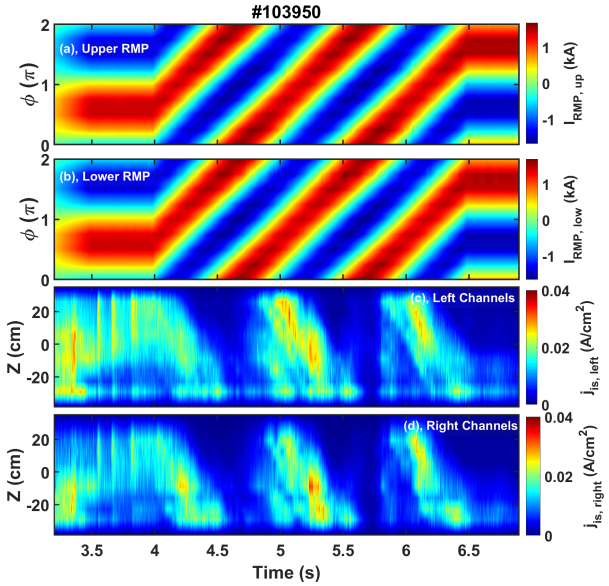

Fig. 9. Temporal evolution of ion saturation current density of LLP array during an RMP experiment. Coil currents of the upper (a) and lower (b) RMP, with the vertical axis as the toroidal angle. Ion saturation current density measured by the left LLP array (a) and the right LLP array (b).

The electron temperature and density measured by LLP channel 12 in a low confinement mode (L-mode) plasma are shown in Fig. 10. The plasma parameters of discharge 103163 are as below: plasma current $I_p = 500$ kA, line-integrated electron density $n_{el} = 1.5\times10^{19}$ m^{-2}, toroidal field 2.47 T at the plasma center, low hybrid wave (LHW) heating power 0.8 MW, and electron cyclotron resonant heating (ECRH) power 1 MW. The feedback control of plasma density is achieved by the SMBI, as shown in the green pulses of Fig. 10 (c). The edge D_α emission intensity increases significantly after the

pulse of SMBI. The LLP channel 12 is operated in the single probe mode and biased with an AC power supply, with the sweep voltage from -210 V to +120 V and a sweep frequency of 500 Hz. The sampling rate of the DAQ system is 1 MHz in this experiment. The electron temperature T_e and ion saturation current I_{is} can be derived from the $I-V$ characteristics by fitting the following equation [37]:

$$I = I_{is}\left[1 - e^{\frac{e(V-V_0)}{kT_e}}\right] \quad \text{for } V < 0 \qquad (1)$$

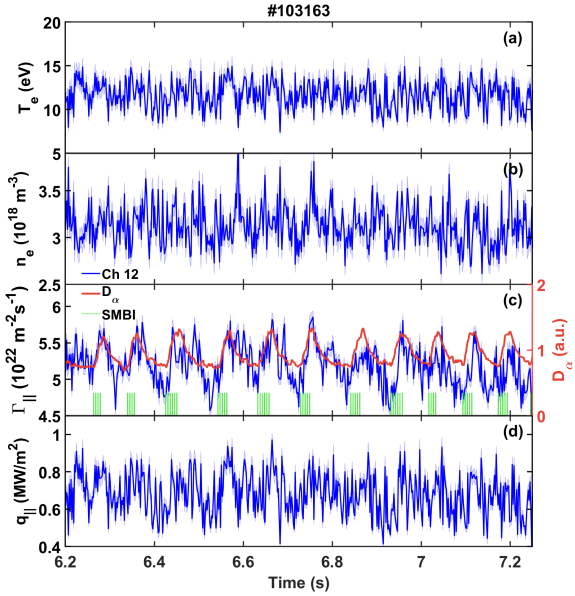

Fig. 10. Plasma parameters measured by the LLP channel 12 in an L-mode plasma. (a) Electron temperature; (b) electron density; (c) particle flux shown in blue, edge D_α emission intensity shown in red, and the pulses of SMBI shown in green; (d) heat flux. The shaded regions of the blue curves denote the error bar of measured parameters.

The fitted electron temperature is presented in Fig. 10 (a), with T_e = 10 – 15 eV, where the error bar is given by the fitting uncertainty. The electron density is derived from the equation $n_e = I_{is}/(0.49eS_{eff}\sqrt{T_e/m_i})$ and shown in Fig. 10 (b) [38], with n_e = 3 – 3.3×10^{18} m^{-3}. The particle flux $\Gamma_\parallel = I_{is}/(eS_{eff})$ is given in Fig. 10 (c), and is modulated significantly by the pulses of SMBI with $\Gamma_\parallel$ = 4.7 – 5.7×10^{22} m^{-2}s^{-1}, i.e., $\Gamma_\parallel$ increases by about 10%. Note that the temporal evolution and amplitude of the fitted ion saturation current I_{is} are consistent with that from the LLP channels operated in Mach probe mode. The heat flux is calculated by $q_\parallel = \gamma k T_e \Gamma_\parallel$, with the sheath transmission coefficient $\gamma = 7$. The heat flux is also modulated by the SMBI pulses in the range of $q_\parallel$ = 0.5 – 0.85 MW/m^2, as illustrated in Fig. 10 (d). The experimental results have demonstrated that the LLP array can measure the temporal evolution of SOL parameters, including T_e, n_e, $\Gamma_\parallel$ and $q_\parallel$, which are essential to study the SOL physics.

4. Summary

A new limiter Langmuir probe array has been developed and applied to the EAST tokamak in 2021. The LLP system contains two poloidal arrays and a totally 52 channels, embedded at the top of the bevel of graphite tiles on the limiter. Each poloidal LLP array has 26 channels and a spatial resolution of 35 mm, and the sampling rate of the DAQ system can be up to 2 MHz, which are high enough to measure the poloidal structure and temporal evolution of the SOL plasma. An LLP consists of graphite tip, copper connector, ceramic holder, spring washer, SS screw, SS nut, connection screw and wire. The electroconductive components (graphite tip, copper connector, connection screw, wire and SS nut) transmitting electric signal are encapsulated in the ceramic holder, and the connections among them are through the bolt-nut method and crimped connection, which is firm and stable. In consequence, the probe electric insulating property is excellent and the measurement is reliable during long-term operation. The probe can be assembled in the laboratory at first and installed in the limiter as a whole. When the assembly is finished, the front probe tip will be polished to match the local graphite tile surface, avoiding sharp leading edge and high heat load. When the probe tip needs maintenance, it can be repaired from the front side during the interval of experimental campaigns. There are three electric circuits for LLP, i.e., floating potential circuit measuring floating potential, Mach probe circuit measuring ion saturation current, single probe circuit measuring electron temperature and density. The circuit setup of the LLP array can be arranged optimally according to the purpose of experimental proposal. Since the edge toroidal magnetic field is much larger than the radial magnetic field, the incident angle of the magnetic field has very weak dependence on the discharge conditions, therefore the effective collecting areas are almost the same for the probes in the circular arc region on limiter. In a commissioning experiment, the ion saturation current density of LLP array exhibits synchronized and cyclic poloidal structure variations with the rotating RMPs, confirming the capability of the LLP array to measure the poloidal structure of SOL plasma with high sensitivity. In another commissioning experiment, the electron temperature and density are measured by a LLP channel that is operated in the single probe mode, and the derived heat and particle fluxes are modulated by the SMBI pulses obviously. This newly developed LLP array will shed more light on the study of divertor-SOL physics, such as the plasma response due to RMP, SOL transport induced by LHW filament and SMBI, and the dynamic process and propagation of ELMs.

Acknowledgement

This work was supported by the National MCF Energy R&D Program (Nos. 2019YFE03040000, 2017YFE0301100, 2017YFE0402500 and 2017YFE0301300), the National Natural Science Foundation of China under grant contract No.

11875294 and 12175277, the Science Foundation of Institute of Plasma Physics, Chinese Academy of Sciences, No. DSJJ-2021-01, the Collaborative Innovation Program of Hefei Science Center, CAS, No. 2021HSC-CIP019, and the Users with Excellence Program of Hefei Science Center, CAS under grant Nos. 2021HSC-UE014.

References

[1] Loarte A. *et al* Chapter 4: Power and particle control, Nucl. Fusion 47 (2007) S203
[2] Federici G. *et al* Plasma-material interactions in current tokamaks and their implications for next step fusion reactors, Nucl. Fusion 41 (2001) 1967
[3] Stangeby P. C. *et al* Plasma Boundary Phenomena in Tokamaks, Nucl. Fusion 30 (1990) 1225
[4] Johnson E. O. *et al* A Floating Double Probe Method for Measurements in Gas Discharges, Phys Rev 80 (1950) 58
[5] Eldon D. *et al* Initial results of the high resolution edge Thomson scattering upgrade at DIII-D, Rev. Sci. Instrum. 83 (2012) 10E343
[6] Schmitz O. *et al* Status of electron temperature and density measurement with beam emission spectroscopy on thermal helium at TEXTOR, Plasma Phys. Control. Fusion. 50 (2008) 115004
[7] Brandenburg R. *et al* Fast lithium beam edge plasma spectroscopy at IPP garching - Status and recent developments, Fusion Technol. 36 (1999) 289
[8] Erents S. K. *et al* Parallel flow in the JET scrape-off layer, Plasma Phys. Control. Fusion. 42 (2000) 905
[9] Asakura N. *et al* Fast reciprocating probe system for local scrape-off layer measurements in front of the lower hybrid launcher on JT-60U, Rev. Sci. Instrum. 66 (1995) 5428
[10] Terry J. L. *et al* The scrape-off layer in Alcator C-Mod: Transport, turbulence, and flows, Fusion Sci. Technol. 51 (2007) 342
[11] Monk R. D., Langmuir probe measurement in the divertor plasma of the JET tokamak, Ph.D. thesis, University of London, 1996.
[12] Buchenauer D. *et al* Langmuir Probe Array for the Diii-D Divertor, Rev. Sci. Instrum. 61 (1990) 2873
[13] Asakura N. *et al* Recycling Enhancement with (N)over-Bar(E) and Q(Eff) in High-Density Discharges on Jt-60u, Nucl. Fusion 35 (1995) 381
[14] Xu J. C. *et al* Upgrade of Langmuir probe diagnostic in ITER-like tungsten mono-block divertor on experimental advanced superconducting tokamak, Rev. Sci. Instrum. 87 (2016) 083504
[15] Ming T. F. *et al* Improvement of divertor triple probe system and its measurements under full graphite wall on EAST, Fusion Eng. Des. 84 (2009) 57
[16] Bak J. G. *et al* Electrical Probe Diagnostics for KSTAR, Contrib. Plasm. Phys. 50 (2010) 892
[17] Hammond K. C. *et al* Drift effects on W7-X divertor heat and particle fluxes, Plasma Phys. Control. Fusion. 61 (2019) 125001
[18] Li Y. L. *et al* Hot spots induced by LHCD in the shadow of antenna limiters in the EAST tokamak, Phys. Plasmas 25 (2018) 082503
[19] Gao X. *et al* Key issues for long-pulse high-beta(N) operation with the Experimental Advanced Superconducting Tokamak (EAST), Nucl. Fusion 57 (2017) 056021
[20] Kirk A. *et al* Spatial and Temporal Structure of Edge-Localized Modes, Phys. Rev. Lett. 92 (2004) 245002
[21] Liang Y. *et al* Active control of type-I edge localized modes with n=1 and n=2 fields on JET, Nucl. Fusion 50 (2010) 025013
[22] Kirk A. *et al* Understanding edge-localized mode mitigation by resonant magnetic perturbations on MAST, Nucl. Fusion 53 (2013) 043007
[23] Fundamenski W. *et al* Radial propagation of type-I ELMs on JET, Plasma Phys. Control. Fusion. 46 (2004) 233
[24] Labombard B. *et al* Densepack - an Array of Langmuir Probes in the Limiter Shadow Plasma of the Alcator-C Tokamak Fusion Experiment, Rev. Sci. Instrum. 57 (1986) 2415
[25] Yang J. *et al* The application of limiter target electrostatic measurement system in J-TEXT tokamak, Plasma Sci. Technol. 21 (2019) 105105
[26] McCormick K. *et al* Core-edge studies with boundary island configurations on the W7-AS stellarator, Plasma Phys. Control. Fusion. 41 (1999) B285
[27] Wenzel U. *et al* Observation of Marfes in the Wendelstein 7-X stellarator with inboard limiters, Nucl. Fusion 58 (2018) 096025
[28] Wan B. N. *et al* Recent advances in EAST physics experiments in support of steady-state operation for ITER and CFETR, Nucl. Fusion 59 (2019) 112003
[29] Liao L. *et al* Physical design of a new set of high poloidal mode number coils in the EAST tokamak, Plasma Science and Technology (2021) submitted
[30] Yao D. M. *et al* EAST in-vessel components design, Fusion Eng. Des. 75-79 (2005) 491
[31] Luo G. N. *et al* Overview of plasma-facing materials and components for EAST, Phys. Scr. T128 (2007) 1
[32] Xu J. C. *et al* Upgrade Design of Lower Divertor Langmuir Probe Diagnostic System in the EAST Tokamak, Ieee T Plasma Sci 46 (2018) 1331
[33] Luo Z. P. *et al* Online Plasma Shape Reconstruction for EAST Tokamak, Plasma Sci. Technol. 12 (2010) 412
[34] Yu L. D. *et al* Development of precision measurement network of experimental advanced superconducting tokamak, Opt Eng 53 (2014) 122406
[35] Xu S. *et al* Mechanism of the active divertor flux control by the supersonic-molecular-beam-injection with lower hybrid wave-induced magnetic perturbations on the EAST tokamak, Nucl. Fusion 60 (2020) 056006
[36] Jia M. *et al* Control of three dimensional particle flux to divertor using rotating RMP in the EAST tokamak, Nucl. Fusion 58 (2018) 046015
[37] Stangeby P. C. Determination of T-e from a Langmuir probe in a magnetic field by directly measuring the probe's sheath drop using a pin-plate probe, Plasma Phys. Control. Fusion. 37 (1995) 1337
[38] Hutchinson I. H. 2002 Principles of plasma diagnostics (Cambridge ; New York: Cambridge University Press), p. 77